Core/shell Eudragit/poly(ethylene oxide) fibers for site-specific release

Dong Jia, Yanshan Gao, and Gareth R. Williams*

UCL School of Pharmacy, University College London, London, WC1N 1AX, UK

* Author for correspondence. Email: g.williams@ucl.ac.uk; tel: +44(0) 207 753 5868

Abstract

Electrospinning was used to prepare core/shell fibers containing the active pharmaceutical ingredients indomethacin (IMC) or mebeverine hydrochloride (MB-HCl). The shell of the fibers was fabricated from the pH sensitive Eudragit S100 polymer, while the drug-loaded core was based on the mucoadhesive polyethylene oxide (PEO). Three different drug loadings (from 9 – 23 % w/w of the core mass) were prepared, and for MB-HCl two different molecular weights of PEO were explored. The resultant fibers generally comprise smooth cylinders, although in some cases defects such as surface particles or flattened or merged fibers were visible. Transmission electron microscopy showed all the systems to have clear core and shell compartments. The drugs are present in the amorphous physical form in the fibers. Dissolution tests found that the fibers can effectively prevent release in acidic conditions representative of the stomach, particularly for the acidic indomethacin. After transfer to a pH 7.4 medium, sustained release over between 6 and 22 h is observed. Given the mucoadhesive nature of the PEO core, after dissolution of the shell the fibers will be able to adhere to the walls of the intestinal tract and give sustained local drug release. This renders them promising for the treatment of conditions such as irritable bowel disease and colon cancer.

Keywords

Coaxial electrospinning; Eudragit S100; core/shell fiber; indomethacin; mebeverine hydrochloride, delayed release

1.   Introduction

Electrospinning is a widely-explored technique for the fabrication of polymer/drug composites. It uses electrical energy to evaporate the solvent from a mixed solution of a polymer and drug. The latter is placed into a syringe fitted with a metal needle tip (the spinneret), and then ejected at a controlled rate towards a metal collector. A large potential difference is applied between the spinneret and the collector, which results in the rapid (*ca.* 10^{-2} s) evaporation of solvent and the formation of a solid composite in the form of one-dimensional fibers, typically with diameters on the nanoscale. Since it avoids the use of heat – common in other manufacturing processes such as spray-drying or hot-melt extrusion – electrospinning offers an attractive approach to handle easily-degradable active ingredients such as proteins (Jiang et al., 2014; Romano et al., 2016). As a result, it has attracted significant attention from pharmaceutical scientists (Persano et al., 2013; Repanas et al., 2016; Sridhar et al., 2015; Zamani et al., 2013).

Electrospun fibers have most commonly been used to develop fast-dissolving drug delivery systems in the form of amorphous solid dispersions. The rapid nature of the spinning process means that the physical form of the fiber-forming components in solution is propagated into the solid state, and hence by preparing fibers from hydrophilic polymers such as poly(vinyl pyrrolidone) dramatic increases in dissolution rate can be achieved (Verreck et al., 2003; Yu et al., 2009). The approach can also be applied in the development of modified release systems, however. In this manifestation, a slow-dissolving or insoluble polymers is used as the filament forming matrix. For instance, Kenawy *et al.* produced fibers of poly(ethylene-co-vinyl acetate), poly(lactic acid), and the antibiotic tetracycline hydrochloride and were able to obtain sustained release over more than 5 days (Kenawy et al., 2002).

Targeted release can also be achieved through use of a pH-sensitive polymer such as the methacrylate-based materials. For instance, the Evonik polymers Eudragit L100-55, L100 and S100 are insoluble below pH 5.5, 6, and 7 respectively, but dissolve freely at pHs above these limits. Fibers made of such materials can preclude drug release in the low-pH environment of the stomach where the polymer is insoluble. The drug is subsequently freed into solution when the fibers enter the higher-pH environment of the small intestine and dissolve. For instance, Eudragit L100 and L100-55 fibers loaded with diclofenac have been prepared, and found to effectively target the small intestine (Shen et al., 2011; Yu et al., 2014). However, it should be noted that simply making a fiber from a pH-sensitive polymer is not in itself sufficient to prevent release at low pH, because the high surface-area-to-volume ratio of the nanoscale fibers produced by electrospinning results in a large proportion of the incorporated drug being present at the surface, and thus easily able to diffuse into the release milieu (Chou et al., 2015; Pelipenko et al., 2015; Sebe et al., 2015; Zupančič et al., 2015).

One strategy that can be used to resolve this problem is to prepare a core/shell fiber through coaxial electrospinning (this uses two needles, one nested inside another, and two independent working solutions).

64 If the shell is drug-free and insoluble at low pH, then release in the acidic medium of the stomach should be

65 avoided. Alas, this has been shown to not always be the case, and it is possible for small molecules in the

66 core to diffuse through the shell even at low pH (Illangakoon et al., 2015). However, in favorable cases, the

67 use of the core/shell architecture can result in systems able to give very precise targeting of drug release. For

68 instance, Jin et al. used coaxial electrospinning to prepared contrast agent loaded fibers for colon-targeted

69 MRI (magnetic resonance imaging) (Jin et al., 2016b). Fibers consisting of poly(ethylene oxide) (PEO) and the

70 contrast agent gadolinium (III) diethylenetriaminepentaacetate hydrate (Gd(DTPA)) as the core, and Eudragit

71 S100 as the shell were prepared. Dissolution studies showed minimal release at pH 1.0, and sustained release

72 over 27 h at pH 7.4. The mucoadhesive properties of the fibers were also measured, and the PEO core showed

73 strong adhesion forces after dissolution of the shell. This work was extended to prepare theranostic

74 Gd(DTPA)/indomethacin/PEO core - Eudragit shell fibers (Jin et al., 2016a). The fibers showed very little drug

75 release at pH 1.0, and sustained release at pH 7.4.

76

77 In this work, we aimed to extend this previous work by preparing core/shell fibers for oral administration and

78 local delivery to the colon. We report a systematic study exploring the role of key formulation parameters on

79 functional performance. The literature is divided as to whether preparing a core/shell fiber with a Eudragit

80 shell is sufficient to prevent release in the stomach or not, and to date there are no systematic studies which

81 directly compare and contrast an acidic and a basic drug in analogous core/shell formulations to determine

82 how the solubility of the drug at low pH affects the release profiles observed. In this work, we remedy this

83 lack of understanding. Further, we seek to explore the effect of the molecular weight of the PEO core on the

84 performance of the systems.

85

86 Oral colon-specific drug delivery systems play an important role in the treatment of colonic diseases such as

87 irritable bowel syndrome (IBS), colon cancer and ulcerative colitis (Nykänen et al., 2001). Local colon specific

88 delivery allows the first pass effect to be bypassed, and releasing the drug at a specific site gives increased

89 local bioavailability and minimizes systemic side effects (Minko, 2004). Two model drugs were selected for

90 exploration: mebeverine hydrochloride and indomethacin. There are several benefits in the local delivery of

91 these, and in addition they have the advantage of comprising a model basic and acidic drug, respectively.

92 Chemical structures are given in **Figure 1**.

93

94
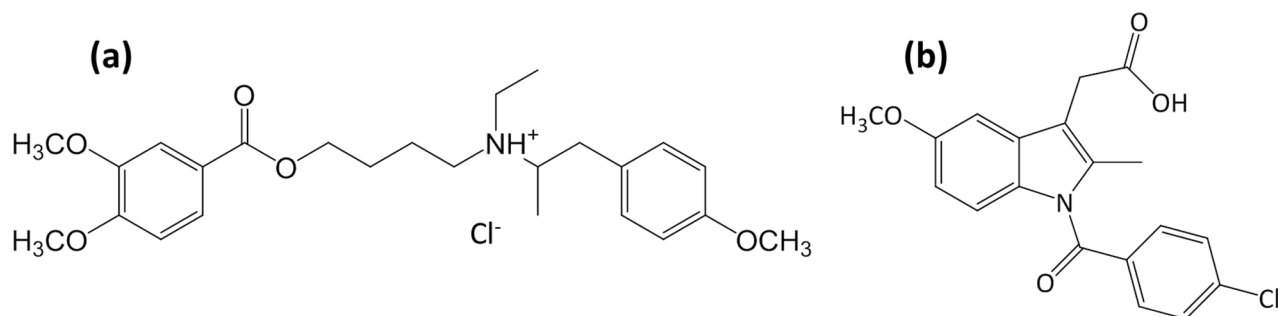
Figure 1: The chemical structures of **(a)** mebeverine hydrochloride and **(b)** indomethacin.

Mebeverine hydrochloride (MB-HCl) is an antispasmodic drug used to treat irritable bowel syndrome (IBS). MB-HCl works through musculotropic activity, and directly acts on the smooth muscles of the colon (Dandagi et al., 2009). However, traditional MB-HCl formulations have a short plasma half-life (2.5h), which means frequent dosing is required for successful treatment (Abdullah et al., 2011). Indomethacin (IMC) is a nonsteroidal anti-inflammatory (NSAID) drug used in the relief of pain and stiffness. Its mechanism of action involves the blocking of cyclooxygenase, which participates in the synthesis of irritant chemicals causing pain (Fitzpatrick, 2004). A number of studies (Hull et al., 2003; Ikawa et al., 2012; Kapitanovic et al., 2006) indicate that IMC can be potent in the treatment of colon cancer. However, it can also cause gastrointestinal bleeding and ulceration (Akhgari et al., 2013). Hence, a colon targeted formulations for IMC would be extremely beneficial to patients.

In this work, we used coaxial electrospinning to prepare core/shell fibers with a Eudragit S100 shell and a PEO core, with the aim of providing colon-targeted delivery. PEO is a highly swellable and mucoadhesive polymer, and after the dissolution of the shell polymer was expected to result in long-lasting drug delivery.

2. Experimental

2.1 Materials

Mebeverine hydrochloride (MB-HCl), indomethacin (IMC), and phosphate buffered saline (PBS) were purchased from Sigma-Aldrich (UK). Two different grades of polyethylene oxide (PEO) were used. PEO with Mw of 400,000 Da was supplied by Sigma-Aldrich (UK), and with Mw of 600,000 Da by Acros Organics (UK). Eudragit S100 was supplied by Evonik GmbH (Germany). Anhydrous ethanol, acetone and hydrochloric acid were purchased from Fisher Scientific (UK). Triton X100 and dimethylacetamide (DMAc) were obtained from Sigma-Aldrich (UK). All water was deionized prior to use.

2.2   Solutions for electrospinning

A shell solution was prepared from 13.5% w/v Eudragit S100 (ES100) dissolved in ethanol and DMAc (2 : 8 v/v). Core solutions were made up in a mixture of ethanol and water (7 : 3 v/v). To aid the spinning process, 1 % v/v acetone and 0.1 % v/v Triton-X 100 were added (Jin et al., 2016b). A series of solutions was prepared as detailed in **Table 1**.

Table 1: The core solutions for coaxial electrospinning.

Solution	PEO Mw / 10^6 Da	PEO conc / % w/v	Drug conc/ mg/mL	Final wt% of drug in the core	Final wt% of drug in the fiber
MB1	0.6	2.5	2.5	9.09	0.36
MB2	0.6	2.5	5	16.67	0.71
MB3	0.6	2.5	7.5	23.08	1.06
MB4	0.4	3	3	9.09	0.42
MB5	0.4	3	6	16.67	0.84
MB6	0.4	3	9	23.08	1.26
IMC1	0.4	3	3	9.09	0.42
IMC2	0.4	3	6	16.67	0.84
IMC3	0.4	3	9	23.08	1.26

Two syringe pumps (KDS100, Cole-Parmer, UK) were employed to independently drive the two working fluids. Solutions were loaded into 5 mL syringes, with care taken to avoid bubbles, and these were then mounted onto the syringe pumps. The coaxial spinneret was supplied by Linari Engineering SRL (Italy), with the inner and outer needles having external/internal diameters of 0.83/0.51 and 1.83/1.37 mm, respectively. The spinneret was connected to the syringes using plastic tubing. A high voltage power supply (HCP 35-35000, FuG Elektronik GmbH, Germany) was connected to the tip of the needle. A flat metal collector was wrapped with aluminum foil and connected to the grounded electrode. The electrospinning process was carried out under ambient conditions at 23 ± 2 °C and 48 ± 12 % relative humidity (RH), at an applied voltage of 10.6 kV. The flow rate for the core solution was 0.3 mL/h, and for the shell solution 1.5 mL/h. The distance from the needle tip to the collector was 20 cm. After collection, fibers were stored in a desiccator over phosphorous pentoxide prior to analysis.

2.3   Characterisation

2.3.1   Electron microscopy

The fibers were first assessed using a scanning electron microscope (Quanta 200, FEI, Netherlands). Prior to examination, samples were sputter coated with a thin layer of gold to render them conductive. The average fiber diameter was quantified from 100 different locations in SEM images, using the ImageJ software. For transmission electron microscopy (TEM), fibers were directly electrospun onto TEM grids. Images were recorded using a CM 120 Bio-Twin instrument (Philips/FEI Corporation, Netherlands).

2.3.2 Differential scanning calorimetry

Differential scanning calorimetry (DSC) analyses were conducted on a Q2000 instrument (TA Instruments, USA). Samples of 4 – 5 mg were accurately weighed into T-zero hermetic aluminum pans, which were subsequently sealed and the lids pinholed. The samples were first heated from 25 to 120 °C, and subsequently cooled to 25 °C. A second heating step was then carried out from 25 to 180 °C. All DSC experiments used a heating rate of 10 °C/min, under a nitrogen purge of 50 mL/min.

2.3.3 X-ray diffraction

X-ray diffraction (XRD) data were acquired using a MiniFlex 600 diffractometer (Rigaku, Japan) with Cu Kα radiation (λ = 1.5418 Å) at 40 kV and 15 mA. Patterns were recorded over the 2θ range 5 to 60° at a scan speed of 5°/min.

2.3.4 Fourier transform infrared spectroscopy

Fourier transform infrared (IR) spectra were recorded using a Spectrum 100 spectrometer (PerkinElmer, USA) fitted with an attenuated total reflectance accessory. The samples were scanned over the range 650 – 4000 cm^{-1}, with resolution of 1 cm^{-1}.

2.3.5 *In* vitro dissolution studies

250 mg of fibers were placed in a metallic sinker. The fiber-loaded sinker was then placed in a buffer solution under 50 rpm continuous stirring at 37 ± 0.5 °C. *In vitro* drug dissolution tests were carried out in 150 mL pH 1.2 hydrochloric acid solution for 2 h, before the fiber-loaded sinkers were transferred to 150 mL of pH 7.4 phosphate buffered saline (PBS) for 22 h. At periodic intervals, 3 mL aliquots were withdrawn from the dissolution medium. The medium was refreshed with 3 mL of preheated fresh buffer solution in order to maintain a constant volume and ensure sink conditions. The drug concentrations in the aliquots were determined using UV spectrometry (6305 spectrophotometer; Jenway, UK), following construction of an appropriate calibration curve. The detection wavelengths were set at 263 nm for MB-HCl and 266 nm for IMC. Experiments were conducted in triplicate and results are reported as mean ± S.D.

2.3.6 Molecular modelling

Molecular modelling was implemented using the HyperChem software (v8.0.10). The structures of mebeverine and indomethacin were first drawn in ChemDraw Professional v15, and a PEO decamer constructed to represent the software. These were then individually imported in HyperChem, hydrogens explicitly included, and a trial 3D structure based on preset bond angles generated. Preliminary geometric minimization was performed with the MM+ forcefield using bond-dipole interactions for the non-bonded electrostatic interactions, and running cycles using a Polak-Ribiere conjugate gradient method until the root mean square (RMS) gradient reached 0.02 kcal/(Å mol). A full energetic minimization then followed using the

187   AMBER3 forcefield. Here, the distance-dependent dielectric constant was assigned a value of 1, and the 1-4

188   scale factors as 0.5 for both electrostatic and van der Waals repulsions. Minimization was undertaken with

189   the Polak-Ribiere conjugate gradient method until the RMS gradient reached 0.001 kcal/(Å mol). No cut-offs

190   were applied with either process, and in both contributions from bond stretching/compressing, bond angle

191   deformations, torsional strain, van der Waals repulsions, H-bonding and electrostatic repulsions were all

192   considered. Once models had been constructed for the drugs and PEO, combinations of these were merged

193   to create drug-polymer composites, which then underwent the same minimization processes.

194

195   3.   Results

196   3.1   Fiber morphology

197   The compositions of the fibers prepared are given in **Table 1**, and SEM images are presented in **Figure 2**.
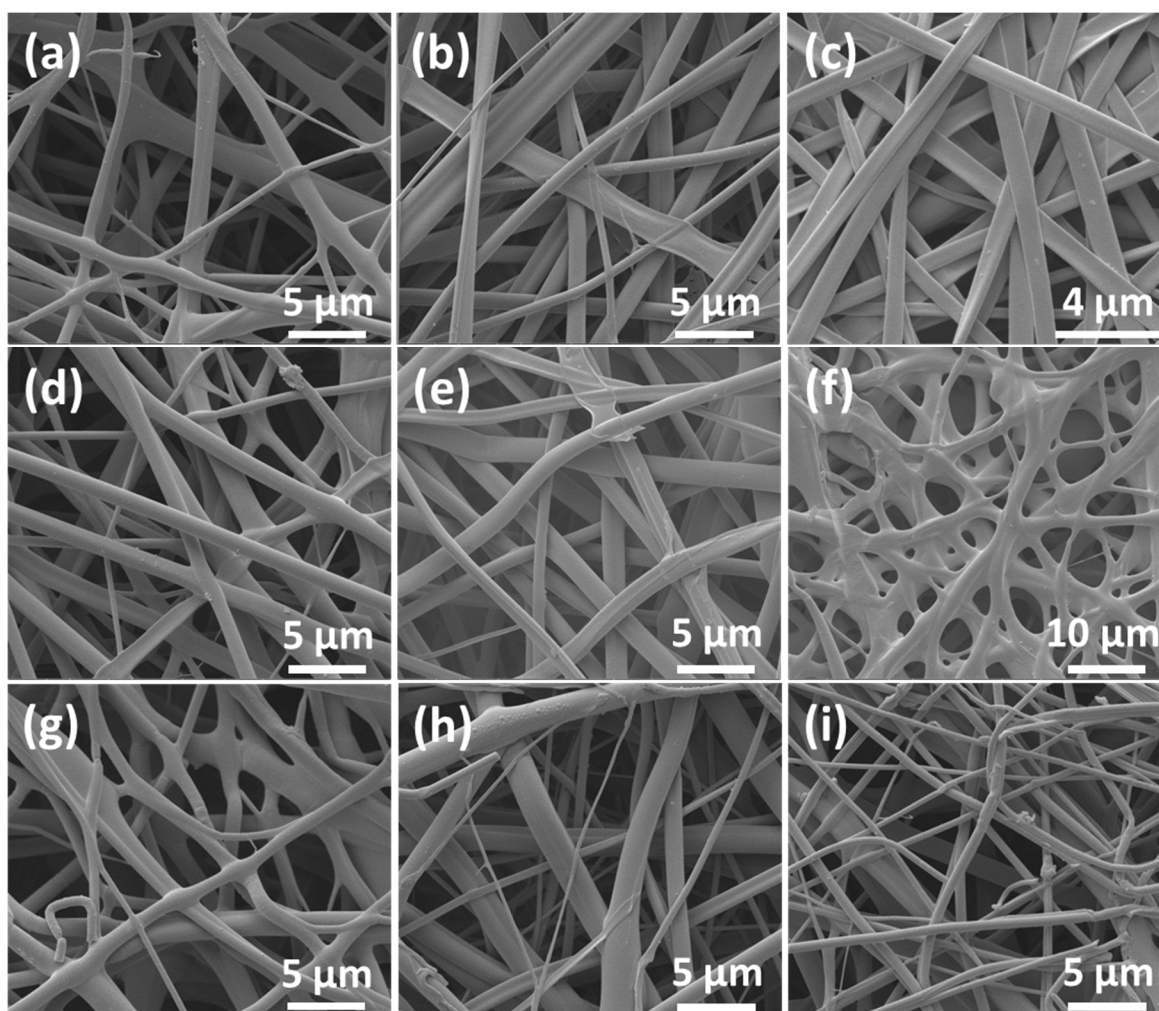
199   **Figure 2:** SEM images of **(a)** MB1; **(b)** MB2; **(c)** MB3; **(d)** MB4; **(e)** MB5; **(f)** MB6; **(g)** IMC1; **(h)** IMC2; and **(i)** IMC3.

200

201   For all the formulations, clear fibers can be seen, although the morphologies are somewhat irregular. The

202   MB1 – 3 systems, prepared with 600 kDa PEO, appear increasingly ribbon-like as the drug concentration

203   increases from 9 to 23 % w/w. This trend is also seen for the MB4 – 6 fibers (made with 400 kDa PEO), and

204   in the high-loading MB6 sample the fibers are clearly merged. No such trends are visible with the IMC

materials. In all cases, a small number of particles can be observed on the surface of the formulations. The fiber diameters are summarised in

Table 2.

Table 2: A summary of the fiber diameters.

| Fiber	Fiber diameter[a] / nm	Approx. core thickness[b] / nm	Approx. shell thickness[b] / nm
MB1	770 ± 370	1110	770
MB2	1100 ± 550	540	860
MB3	770 ± 240	270	265
MB4	910 ± 460	450	1250
MB5	1190 ± 410	1375	1130
MB6	1270 ± 530	1205	1005
IMC1	930 ± 420	780	1270
IMC2	820 ± 590	330	390
IMC3	740 ± 410	255	870

[a] Measured from the SEM images in Figure 2.
[b] Estimated from the mean values in the TEM images in Figure 3

The diameters are all around 1 μm. There are no clear trends in size for MB1 – 3. For MB4 – 6 the size increases with the drug loading, while with the IMC fibers the opposite trend is observed and the diameters decrease with increasing drug loading. These observations can presumably be explained by changes in the viscosity and conductivities of the solutions upon the addition of active ingredient.

TEM images are presented in **Figure 3**. A clear core/shell structure is visible in all cases, despite some inhomogeneities in the fiber diameters and morphologies. This demonstrates that the arrangement of materials in the spinneret has been successfully propagated into the fiber products. The thicknesses of the core and shell compartments are summarised in **Table 2**; because of the small sample size, there are some differences between the values obtained and the overall diameters determined from SEM. The latter are much more accurate, since they are calculated on the basis of more than 100 data points.
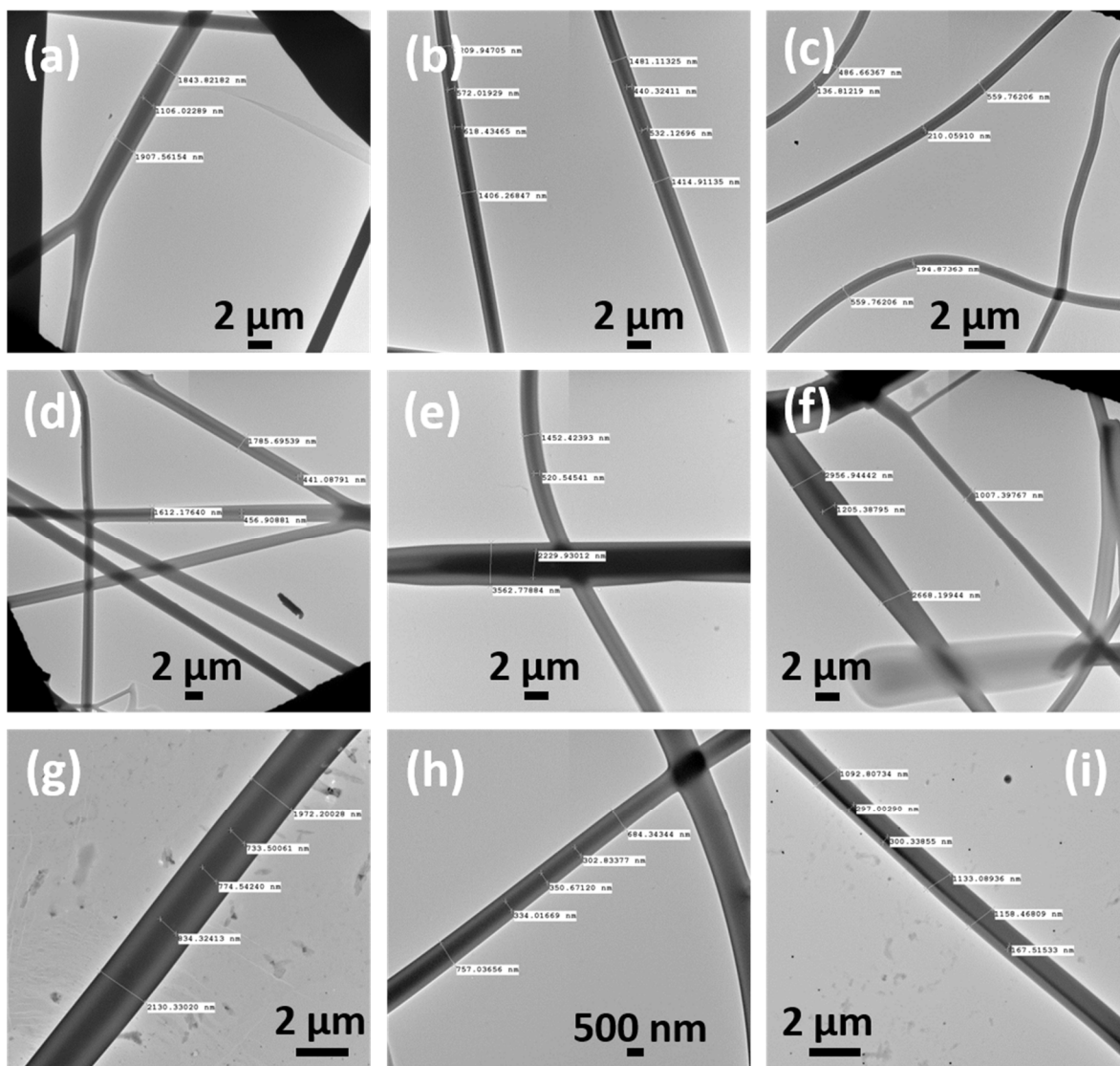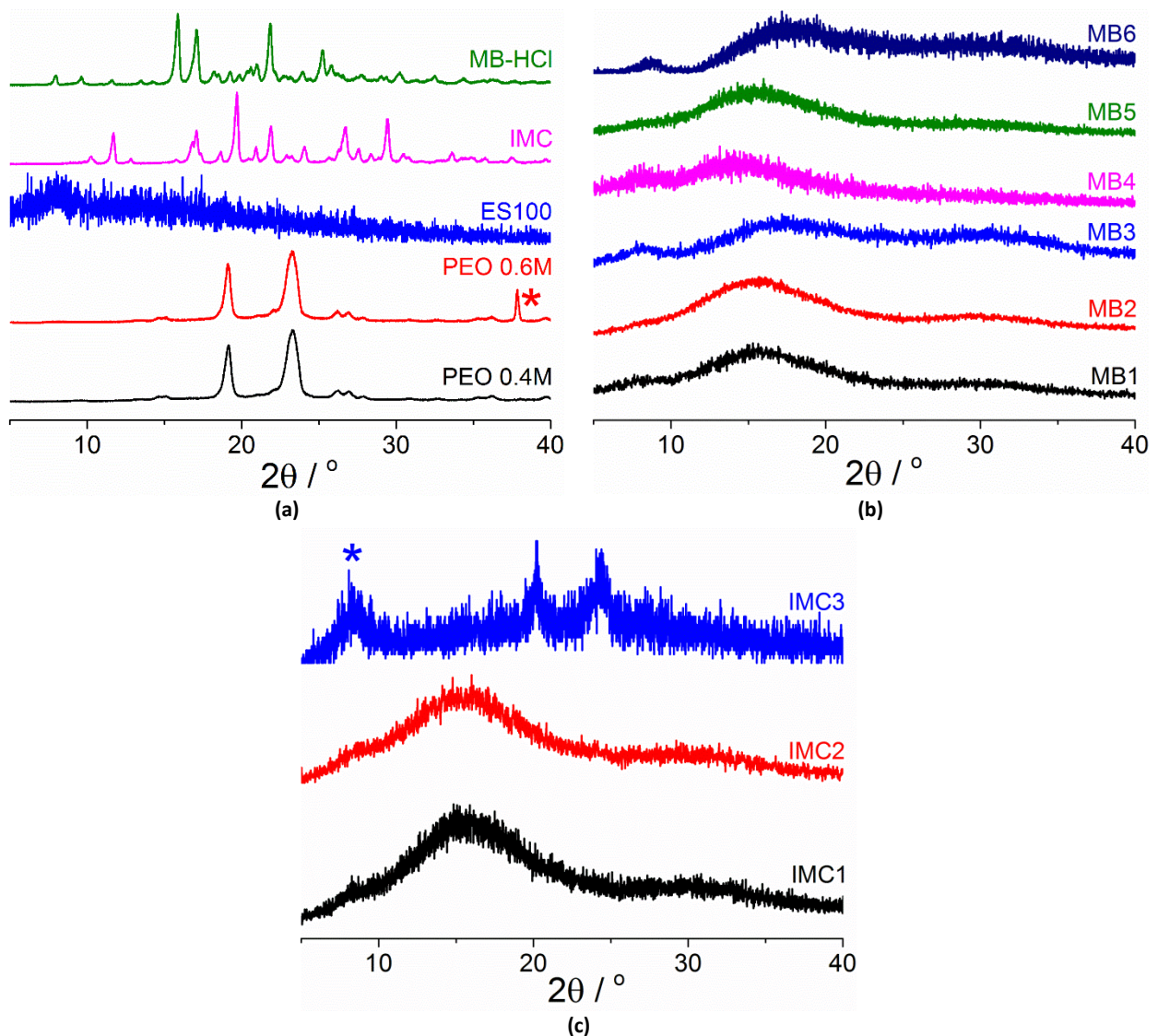
Figure 3: TEM images of **(a)** MB1; **(b)** MB2; **(c)** MB3; **(d)** MB4; **(e)** MB5; **(f)** MB6; **(g)** IMC1; **(h)** IMC2; and **(i)** IMC3.

3.2   Physical form and component compatibility

The physical form of the drug in the fibers was investigated using X-ray diffraction (XRD) and differential scanning calorimetry (DSC). XRD results are given in **Figure 4**.
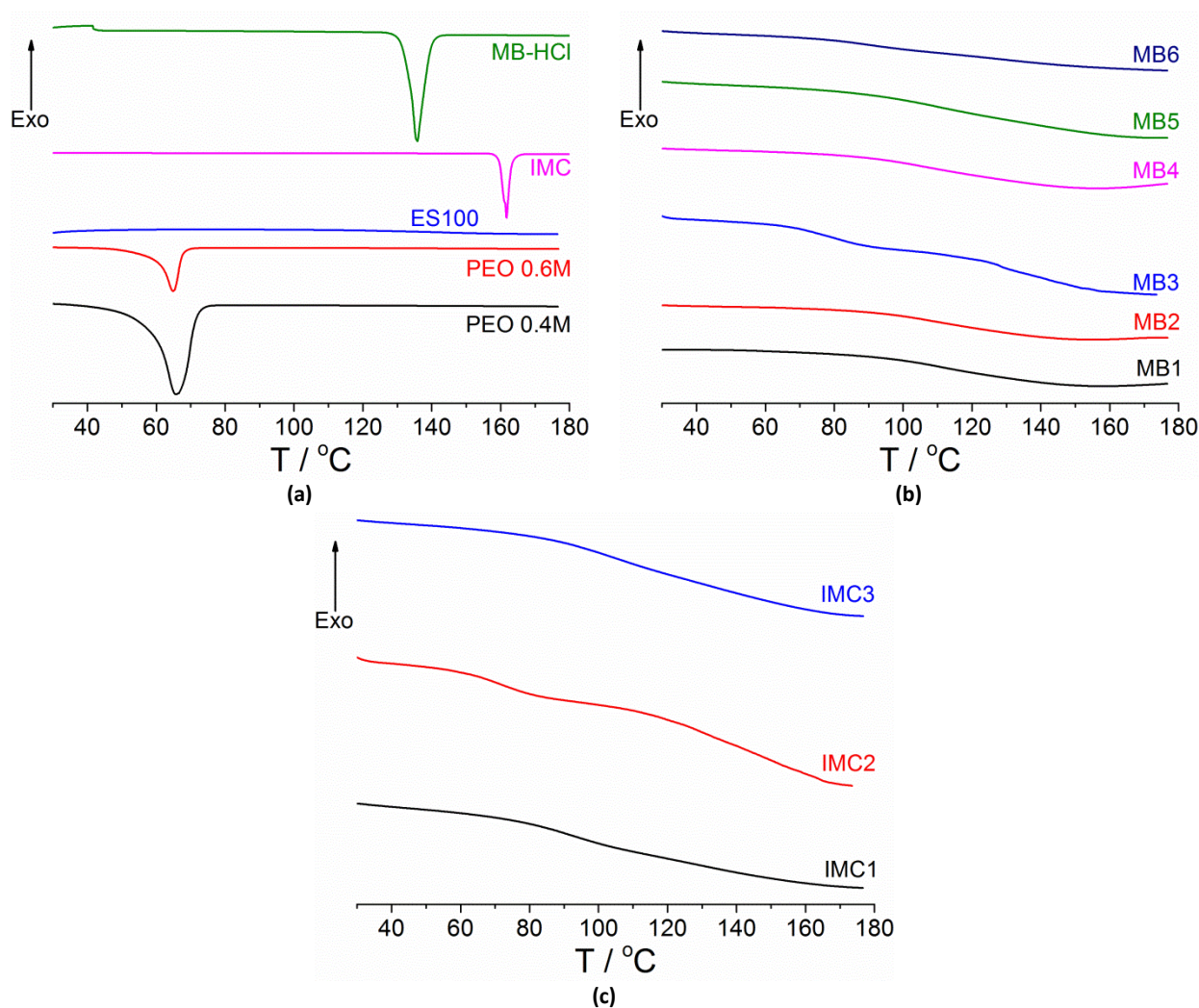
Figure 4: XRD data for the raw materials and fibers, showing: **(a)** the starting materials; **(b)** the MB-HCl formulations; and, **(c)** the IMC fibers. Peaks marked * correspond to the sample holder.

The pure drugs are both clearly crystalline materials, as evidenced by the presence of a large number of distinct Bragg reflections in their diffraction patterns. Both grades of PEO are semi-crystalline, with two broad reflections at 19 and 23°. ES100 is an amorphous material, and therefore only broad humps are observed in its pattern. The MB fibers all show a complete absence of Bragg reflections in their XRD patterns, and hence it can be concluded that the drug and PEO have been rendered into the amorphous form through electrospinning. The fibers exist as amorphous solid dispersions, as has been reported previously by a number of authors (Illangakoon et al., 2014; Jin et al., 2016a; Lopez et al., 2014; Zamani et al., 2013). The same is true for the IMC1 and IMC2 fibers. The picture is more complex for IMC3, and it appears that some crystalline PEO may be present in this formulation, given the presence of broad peaks at 20 and 24°.

Figure 5: DSC data for the raw materials and fibers, showing: **(a)** the starting materials; **(b)** the MB-HCl formulations; and, **(c)** the IMC fibers. Data are shown from the second heating cycle.

The DSC data (**Figure 5**; second heats are shown) concur well with the findings from XRD. MB-HCl is a crystalline material with a melting endotherm at 135 °C, as is IMC (which melts at 161 °C). The former is consistent with the literature melting point for MB-HCl (Illangakoon et al., 2014), while the latter is consistent with the γ-polymorph of IMC (Surwase et al., 2013). Both grades of PEO (0.4M and 0.6M) are semi-crystalline materials with melting points at 64 °C and 65 °C, respectively. ES100 displayed a gradual change in baseline from around 90 to 160 °C, likely to be because of its glass transition at around 143 °C (Jin et al., 2016a). Melting endotherms are not visible in any of the MB-HCl formulations, suggesting MB-HCl is amorphous in all the fibers. Similar findings are noted for IMC: none of the IMC formulations show any melting endotherms, and thus the fibers appear to be amorphous solid dispersions. All the fiber formulations exhibit a broad shift at around 140 °C, which may be due to the glass transition of ES100 in line with previous work (Jin et al., 2016a).

There is a small disconnect in the data for IMC3, where the DSC data indicates a fully amorphous system while the XRD suggests there might be some crystalline PEO remaining. This arises because the DSC data are

260   from the second heating cycle; the samples were first heated from room temperature to 120 °C to remove

261   any residual water and allow other events to be clearly seen. This will not affect any crystalline IMC or MB-

262   HCl which might have been present, since their melting points are above this temperature, but any crystalline

263   PEO will have melted during this heat. There is evidence from the first heating cycle (data not shown) of a

264   very broad endotherm centered at ca. 75 °C which may be consistent with PEO melting, but this cannot be

265   clearly distinguished from dehydration events. We believe that crystalline PEO present at the start of the DSC

266   experiment did not recrystallize during the subsequent cooling/heating cycles, and thus no melt endotherm

267   is seen. Alternatively, it could be that very poorly crystalline PEO is present in IMC3 even after reheating, but

268   the melt endotherms are very broad and so cannot be discerned from the baseline. Overall therefore, the

269   DSC and XRD data together clearly demonstrate that the formulations comprise amorphous solid dispersions,

270   except for IMC3 where a small amount of crystalline PEO is thought to be present.

271

272   IR spectra are shown in **Figure 6**. The raw materials are presented first, in Figure 6(a). The spectrum of MB-

273   HCl contains a broad peak at *ca.* 2450 cm^{-1}, corresponding to N^{+}–H stretching. There are further bands at

274   1717 cm^{-1} (C=O stretching), 1510 cm^{-1} (C=C groups in the benzene rings), and a series of bands around 2950

275   cm^{-1} (aromatic and aliphatic C–H stretching).The spectrum of Eudragit S100 showed characteristic bands at

276   1726 cm^{-1} (C=O stretching vibrations) and 1150 cm^{-1} (corresponding to C-O stretching). The PEO materials

277   exhibit bands at ca. 2875 cm^{-1}, arising from aliphatic C-H stretching, and at 1093 cm^{-1} from the C-O-C groups.

278   Finally, IMC possesses particularly distinct bands at just below 3000 cm^{-1} (C-H stretches) and 1689 and 1713

279   cm^{-1} (C=O groups).

280

281
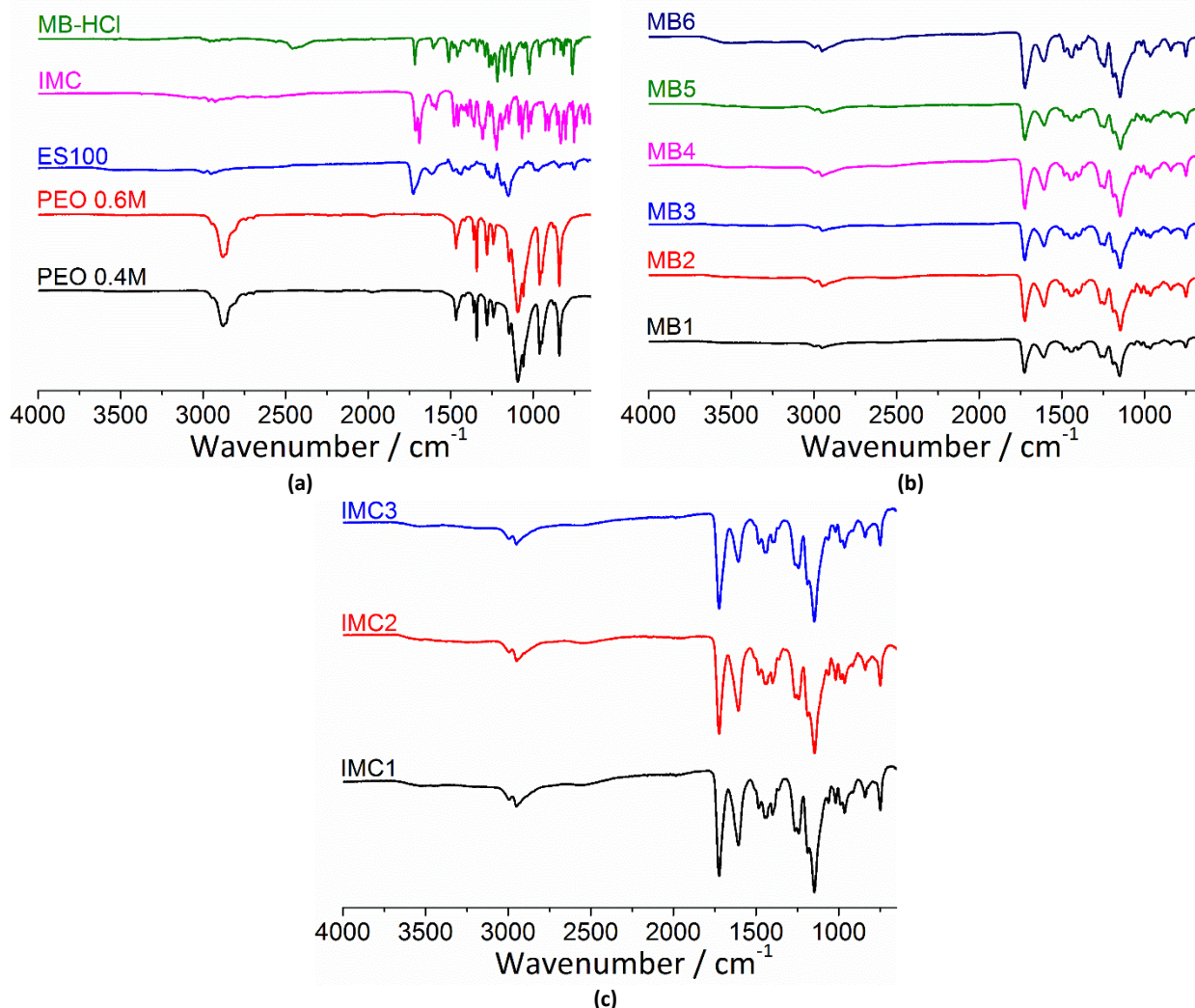
Figure 6: IR spectra of (a) the raw materials; (b) the MB-HCl fibers; and (c) the IMC-loaded materials.

As would be expected, the drug-loaded fibers have spectra which largely comprise composites of their raw materials. However, there are some differences between the spectra of the pure drug and polymer and those of the drug-loaded fibers. For all the MB-HCl containing fibers, the characteristic band of MB-HCl at 2475 cm^{-1} (N$^+$–H stretch) is absent. This situation was also described by Illangakoon and co-workers in their work on MB-HCl loaded PVP and Eudragit fibers (Illangakoon et al., 2014). The disappearance of this peak could be explained by partial proton transfer from the MB-HCl to other components of the fibers, but given the low drug content in the fibers this absence may simply be a result of the limit of detection of the instrument (this peak also cannot be seen in physical mixtures made with the same proportions of ingredients as the fibers, where no interactions should be present). The 1717 cm^{-1} (C=O stretching) peak of MB-HCl is also shifted to 1724 – 1726 cm^{-1}, while the peak at 1510 cm^{-1} (which is still visible in physical mixtures; data not shown) cannot be seen in the fiber spectra. In the IMC case, the C=O bands have shifted to 1607 and 1724 cm^{-1},

296 merging with peaks from the PEO 0.6M. These changes could indicate the formation of intermolecular

297 interactions, but this cannot be determined with certainty owing to the low drug loading of the systems.

298

299 Since it did not prove possible to confirm the presence of intermolecular interactions by IR spectroscopy, we

300 constructed some simple molecular models to gain further insight. The energies of mebeverine, IMC, and a

301 PEO decamer were first minimized, with values given in **Table 3**. Next, we combined the energy-minimized

302 structures of mebeverine or IMC and PEO to create drug polymer complexes, and minimized the energies of

303 these complexes (**Table 3**). The geometric preferences for PEO-IMC and PEO-indomethacin are given in

304 **Figure 7**. Calculation of the difference (ΔE) between the total steric energy of the PEO-drug complexes and

305 the sum of the total steric energies of the individual molecules provides some insight into the intermolecular

306 interactions present. In both cases, ΔE is negative, confirming the presence of favourable interactions (van

307 der Waals and H-bonding) between the drug and polymer (see **Table 3**).

308

309 **Table 3:** The energetics of the optimised geometries in the PEO-drug composites. The electrostatic contribution was found to be 0 in
310 all cases.

Species	Energy / kcal mol^{-1}						
	Bond-stretching	Bond angle	Torsional	van der Waals	H-bonding	Total	ΔE[a]
IMC	0.6280	13.3723	7.1101	3.1252	-1.53E-05	24.2356	-
Mebeverine	1.3441	6.7667	3.1217	10.7141	0	21.9466	-
PEO	0.2782	1.2603	10.0032	5.5913	-0.0017	17.1313	-
PEO-IMC	0.9141	14.7566	17.8620	-2.5773	-0.0187	30.9367	-10.4303
PEO-mebeverine	1.5705	8.2259	13.8529	3.3278	-0.0017	26.97557	-12.1025

311 [a] ΔE = Energy of PEO-drug composite – [energy of drug + energy of PEO]
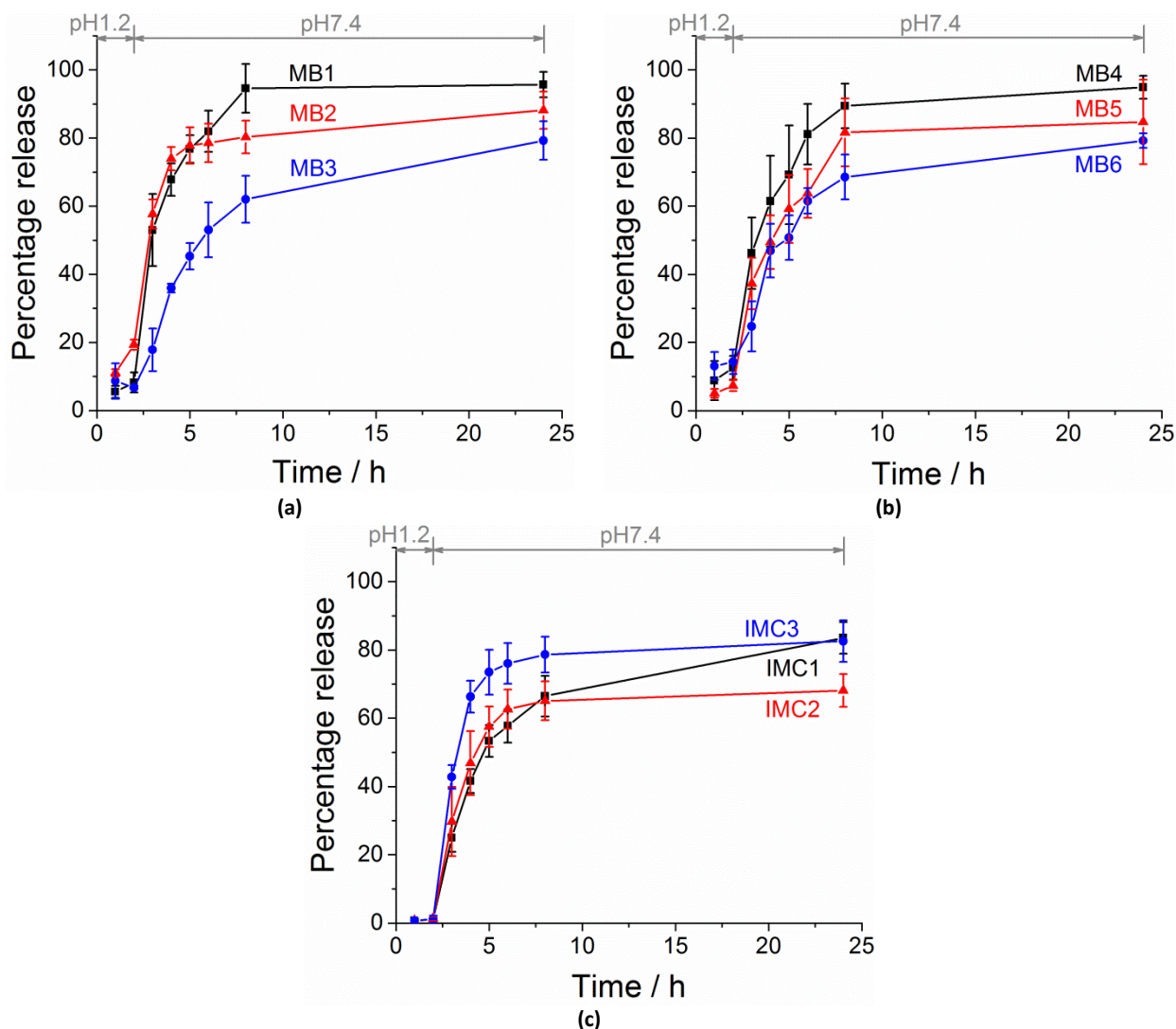
312

313
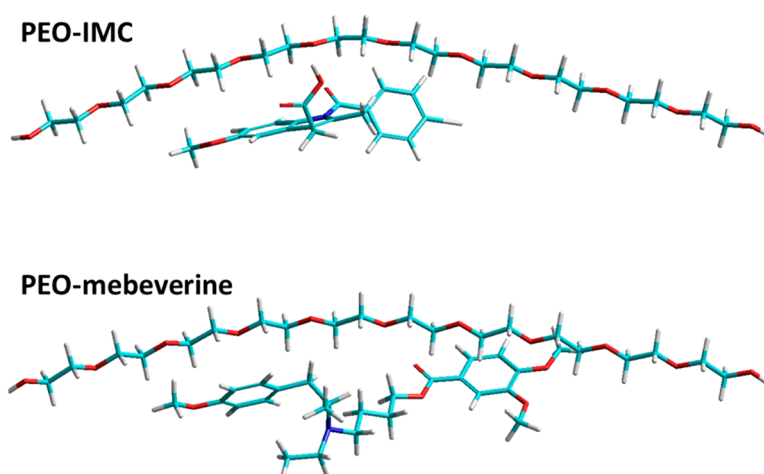
314
315

316 **Figure 7:** The energy-minimized structures of the PEO-IMC and PEO-mebeverine complexes.

317

318 ## 3.3 Dissolution studies

319 Dissolution experiments were performed in an HCl solution at pH 1.2 for 2h, after which the fibers were

320 transferred to a pH 7.4 buffer for another 22h. The results are depicted in **Figure 8**.

321

(a)

(b)

(c)

322 **Figure 8:** *In vitro* release profiles for **(a)** MB1, MB2, and MB3, made with PEO 0.4M; **(b)** MB4, MB5, and MB6, prepared with PEO
323 0.6M; and, **(c)** IMC1, IMC2, and IMC3, made with PEO 0.4M.

324 The release profiles are all relatively similar: there is initially a small amount of release in the acidic buffer,

325 after which there is relatively rapid release for the next 6 – 22 h. It is clear that the ES100 coating effectively

326 prevents release below pH 7. After 8h, the IMC systems have generally reached a plateau, but release

327 continues after this time for IMC1 and the MB-HCl systems. A summary of the release data is given in **Table**

328 **4**.

329

330

331

Table *4*: A summary of some key parameters from *in vitro* dissolution experiments.

Fiber	Release after 2 h / %	Release after 8 h / %	Max. extent of release / %
MB1	8.2 ± 2.9	94.6 ± 7.1	95.7 ± 3.7
MB2	19.4 ± 1.5	80.3 ± 4.8	88.2 ± 5.5
MB3	6.8 ± 0.6	62.0 ± 6.9	79.3 ± 5.6
MB4	12.6 ± 3.4	89.4 ± 6.5	94.9 ± 3.4
MB5	7.4 ± 1.6	81.7 ± 10.0	84.7 ± 12.4
MB6	14.3 ± 3.6	68.6 ± 6.5	79.2 ± 2.1
IMC1	1.2 ± 0.3	66.5 ± 5.9	83.5 ± 4.6
IMC2	1.3 ± 0.7	65.1 ± 5.7	68.1 ± 4.8
IMC3	1.1 ± 1.0	78.7 ± 5.3	82.6 ± 6.1

333

334   As would be expected, the IMC fibers release much less of their drug loading in the HCl buffer than the MB-

335   HCl analogues. This is a result of IMC being an acidic drug, which has minimal solubility at pH 1.2, while the

336   basic MB-HCl is more soluble here. The US Pharmacopoeia states that for delayed release dosage forms, less

337   than 10% of the incorporated drug should be released in the acidic media. Other than MB2, MB4 and MB6,

338   all the materials meet this specification. There are no clear trends between the drug release at pH 1.2 and its

339   loading or the molecular weight of PEO used. All the formulations exhibit some drug particles at their surfaces

340   in SEM (see **Figure 2**), which might be expected to contribute to release at low pH where the ES100 shell is

341   not soluble; however, not all show appreciable release at pH 1.2. Thus, the presence of these defects is not

342   thought to be of great importance.

343

344   After 6 h in a pH 7.4 phosphate buffer, between 62 and 94.6 % of the incorporated drug has been released

345   for MB-HCl. For IMC the range is 65.1 – 78.7 %. In the MB-HCl case, it appears that an increase in the drug

346   content reduces the amount of drug released after 8 h, and this trend is still observed at the 24 h timepoint

347   (see **Table 3**). This might be explained considering the basic nature of the drug, and the fact that as its w/w

348   content in the fibers increases there is less polymer present to aid solubilisation in neutral conditions. The

349   molecular weight of PEO used does not appear to make any appreciable difference to the release profiles.

350

351   Considering the IMC data, it can be seen that IMC2 releases less drug than the other two formulations after

352   24 h. It is not clear why this arises, but may be the result of there being much increased solubilisation from

353   the PEO excipient in the core of IMC1 (9.09 % IMC), and the relatively high solubility of the indomethacin at

354   pH 7.4 in IMC3 (23.08 % IMC). It may be that in IMC2 both of these dissolution enhancing effects are

355   attenuated by the intermediate proportions of both drug and polymer.

356

357   Attempts were made to analyse the data with the Korsmeyer-Peppas equation (data not shown). In a number

358   of cases, there were insufficient datapoints below 60 % release for this to be meaningful, but where analysis

359   could be attempted the results were clearly non-linear plots. This can be ascribed to the Korsmeyer-Peppas

360   equation assuming a uniform distribution of active ingredient throughout the formulation, which is clearly

361   not the case for the core-shell fibers prepared in this work.

362

4.   Discussion

This work builds on the earlier findings of Jin et al. (Jin et al., 2016a), who reported core/shell PEO/indomethacin/Gd(DTPA)-Eudragit materials and used these to simultaneously delivery IMC as a model drug, and Gd(DTPA) for MRI imaging. Similar to this work, they find minimal release of the drug (< 10 %) at pH 1.2, and then sustained release over the next 8 – 29 h. Jin used PEOs with molecular weights of 600 and 1000 kDa in their work, and here we extend this to show that PEO of 400 and 600 kDa can be used to prepare drug-loaded core/shell fibers with a pH sensitive exterior.

There have been a number of reports recently concerning Eudragit-based fibers, with some also employing core/shell architectures. The majority of these studies show minimal release at low pH, even when using monolithic Eudragit L100 or S100 fibers (Aguilar et al., 2015; Illangakoon et al., 2014; Karthikeyan et al., 2012; Shen et al., 2011; Yu et al., 2013a; Yu et al., 2013b). In general, these studies have employed acidic or non-ionisable but highly insoluble drugs, which perhaps goes some way to explaining the efficiency of monolithic Eudragit-based fibers – intuitively, a significant proportion of release would be expected at low pH if the drug is soluble in those conditions, given the very high surface area of the fibers will lead to much of the drug being present at the fiber surface. Illangakoon et al. have recently reported the preparation of fibers with a Eudragit S100 shell, and a 5-fluorouracil-loaded core (Illangakoon et al., 2015). Regardless of the polymer used for the core, these systems showed appreciable amounts of release at pH 1, which was ascribed to the relatively high solubility of the drug under these conditions, and also its low molecular weight helping it to permeate through pores in the fiber shell and into solution.

In this work, we sought to understand in more detail how the acidic or basic nature of the incorporated drug, and the molecular weight of the PEO core, affect release from core/shell PEO/Eudragit fibers. The fibers prepared here indicate that, when working with larger molecular weight drugs (466 g mol^{-1} for MB-HCl and 358 g mol^{-1} for IMC, as compared to 131 g mol^{-1} for 5-fluorouracil), the production of fibers with a Eudragit S100 sheath can be effective in reducing drug release. It is clear that the basic drug MB-HCl is freed to a greater extent in the initial, low-pH, phase of the release experiment than the acidic IMC, but drug release is always < 20 % whereas in Illangakoon's work values up to ca. 80 % were observed (Illangakoon et al., 2015). Hence, although the ionisability of the drug does influence the release profiles, even with a basic drug it is possible to largely prevent release in the low pH conditions of the stomach. The molecular weight of the PEO in the core does not appear to have any major effect on the release profile, and hence there is scope to use a wide range of different grades of this polymer in the core.

In terms of the fibers' potential for direct exploitation as medicines, the drug loadings (at around 0.4 – 1.25 % w/v) are rather too low for application: for MB-HCl a typical treatment regimen is 135 mg three times daily,

398 while that of IMC might be 20 – 40 mg three times daily. Further work is thus required to increase the loading

399 in order to yield suitable formulations for clinical use; this will form the focus of our future work.

400

401 Overall, it is clear from the data presented in this work that these types of formulations have potential for

402 colon-targeted delivery if the active ingredient is chosen with care. The mucoadhesive nature of the PEO core

403 (explored in detail in previous work by Jin, and found to be preserved after electrospinning and dissolution

404 of the shell ES100 (Jin et al., 2016b)) should permit the formulations to adhere to the intestinal wall after

405 dissolution of the Eudragit shell, thereby permitting long-term delivery of either MB-HCl or IMC. Local action

406 on the intestinal wall is required for MB-HCl to have efficacy, and would also be beneficial for IMC in the

407 treatment of colon cancer. Therefore, we believe these formulations may offer new modalities for the

408 treatment of irritable bowel syndrome or cancer.

409

410 **5.   Conclusions**

411 In this work, we report the preparation of a series of nine new formulations, six of mebeverine hydrochloride

412 and three of indomethacin. These comprise electrospun fibers with a pH-sensitive Eudragit S100 shell and a

413 drug-loaded polyethylene oxide (PEO) core. The fibers are found to be largely cylindrical, with smooth

414 surfaces in general, although some particles at the surface and flattened or merged fibers are visible.

415 Transmission electron microscopy was employed to confirm that all the fibers have clear core/shell

416 structures. The drugs are found to be distributed in the amorphous physical form in the formulations.

417 Dissolution tests revealed that the fibers are able to effectively preclude drug release in a pH 1.2

418 environment, particularly in the case of the acidic drug indomethacin. Sustained release over *ca.* 6 – 22 h

419 then ensues at pH 7.4. Given the mucoadhesive nature of the PEO core, the core of the fibers will have the

420 ability to adhere to the wall of the intestinal tract after dissolution of the shell, providing long-term local

421 delivery of either indomethacin or mebeverine. These formulations could hence offer new treatments for

422 irritable bowel syndrome or colon cancer, where local drug application is required.

423

424 **6.   Acknowledgements**

428

429 **7.   References**

430 Abdullah, G.Z., Abdulkarim, M.F., Chitneni, M., Mutee, A.F., Ameer, O.Z., Salman, I.M., Noor, A.M., 2011.
431 Preparation and in vitro evaluation of mebeverine HCl colon-targeted drug delivery system. Pharm. Dev.
432 Tech. 16, 331-342.

433 Aguilar, L.E., Unnithan, A.R., Amarjargal, A., Tiwari, A.P., Hong, S.T., Park, C.H., Kim, C.S., 2015. Electrospun
434 polyurethane/Eudragit(R) L100-55 composite mats for the pH dependent release of paclitaxel on duodenal
435 stent cover application. Int. J. Pharm. 478, 1-8.

436 Akhgari, A., Heshmati, Z., Sharif Makhmalzadeh, B., 2013. Indomethacin electrospun nanofibers for colonic
437 drug delivery: preparation and characterization. Adv. Pharm. Bull.3, 85-90.

438 Chou, S.F., Carson, D., Woodrow, K.A., 2015. Current strategies for sustaining drug release from electrospun
439 nanofibers. J. Control. Release 220, 584-591.

440 Dandagi, P., Mastiholimath, V., Gadad, A., Kulkarni, A., Konnur, B., 2009. pH-sensitive mebeverine
441 microspheres for colon delivery. Indian J. Pharm. Sci. 71, 464-468.

442 Fitzpatrick, F., 2004. Cyclooxygenase enzymes: regulation and function. Current Pharm. Des. 10, 577-588.

443 Hull, M.A., Gardner, S.H., Hawcroft, G., 2003. Activity of the non-steroidal anti-inflammatory drug
444 indomethacin against colorectal cancer. Cancer Treat. Rev. 29, 309-320.

445 Ikawa, Y., Fujino, H., Otake, S., Murayama, T., 2012. Indomethacin antagonizes EP(2) prostanoid receptor
446 activation in LS174T human colon cancer cells. Eur. J. Pharmacol. 680, 16-21.

447 Illangakoon, U.E., Nazir, T., Williams, G.R., Chatterton, N.P., 2014. Mebeverine-loaded electrospun
448 nanofibers: physicochemical characterization and dissolution studies. J. Pharm. Sci. 103, 283-292.

449 Illangakoon, U.E., Yu, D.G., Ahmad, B.S., Chatterton, N.P., Williams, G.R., 2015. 5-Fluorouracil loaded Eudragit
450 fibers prepared by electrospinning. Int. J. Pharm. 495, 895-902.

451 Jiang, H., Wang, L., Zhu, K., 2014. Coaxial electrospinning for encapsulation and controlled release of fragile
452 water-soluble bioactive agents. J. Control. Release 193, 296-303.

453 Jin, M., Yu, D.G., Geraldes, C.F., Williams, G.R., Bligh, S.W., 2016a. Theranostic fibers for simultaneous imaging
454 and drug delivery. Mol. Pharm. 13, 2457-2465.

455 Jin, M., Yu, D.G., Wang, X., Geraldes, C.F., Williams, G.R., Bligh, S.W., 2016b. Electrospun contrast-agent-
456 loaded fibers for colon-targeted MRI. Adv. Healthcare Mater. 5, 977-985.

457 Kapitanovic, S., Cacev, T., Antica, M., Kralj, M., Cavric, G., Pavelic, K., Spaventi, R., 2006. Effect of
458 indomethacin on E-cadherin and beta-catenin expression in HT-29 colon cancer cells. Exp. Mol. Path. 80, 91-
459 96.

460 Karthikeyan, K., Guhathakarta, S., Rajaram, R., Korrapati, P.S., 2012. Electrospun zein/eudragit nanofibers
461 based dual drug delivery system for the simultaneous delivery of aceclofenac and pantoprazole. Int. J. Pharm.
462 438, 117-122.

463 Kenawy, E.-R., Bowlin, G.L., Mansfield, K., Layman, J., Simpson, D.G., Sanders, E.H., Wnek, G.E., 2002. Release
464 of tetracycline hydrochloride from electrospun poly(ethylene-co-vinylacetate), poly(lactic acid), and a blend.
465 J. Control. Release 81, 57-64.

466 Lopez, F.L., Shearman, G.C., Gaisford, S., Williams, G.R., 2014. Amorphous formulations of indomethacin and
467 griseofulvin prepared by electrospinning. Mol. Pharm. 11, 4327-4338.

468 Minko, T., 2004. Drug targeting to the colon with lectins and neoglycoconjugates. Adv. Drug Del. Rev. 56,
469 491-509.

470 Nykänen, P., Lempää, S., Aaltonen, M.L., Jürjenson, H., Veski, P., Marvola, M., 2001. Citric acid as excipient in
471 multiple-unit enteric-coated tablets for targeting drugs on the colon. Int. J. Pharm. 229, 155-162.

472 Pelipenko, J., Kocbek, P., Kristl, J., 2015. Critical attributes of nanofibers: preparation, drug loading, and tissue
473 regeneration. Int. J. Pharm. 484, 57-74.

474 Persano, L., Camposeo, A., Tekmen, C., Pisignano, D., 2013. Industrial upscaling of electrospinning and
475 applications of polymer nanofibers: A review. Macromol. Mater. Eng. 298, 504-520.

476 Repanas, A., Andriopoulou, S., Glasmacher, B., 2016. The significance of electrospinning as a method to
477 create fibrous scaffolds for biomedical engineering and drug delivery applications. J. Drug Del. Sci. Technol.
478 31, 137-146.

479 Romano, L., Camposeo, A., Manco, R., Moffa, M., Pisignano, D., 2016. Core-shell electrospun fibers
480 encapsulating chromophores or luminescent proteins for microscopically controlled molecular release. Mol.
481 Pharm. 13, 729-736.

482 Sebe, I., Szabo, P., Kallai-Szabo, B., Zelko, R., 2015. Incorporating small molecules or biologics into nanofibers
483 for optimized drug release: A review. Int. J. Pharm. 494, 516-530.

484 Shen, X., Yu, D., Zhu, L., Branford-White, C., White, K., Chatterton, N.P., 2011. Electrospun diclofenac sodium
485 loaded Eudragit(R) L 100-55 nanofibers for colon-targeted drug delivery. Int. J. Pharm. 408, 200-207.

486   Sridhar, R., Lakshminarayanan, R., Madhaiyan, K., Amutha Barathi, V., Lim, K.H., Ramakrishna, S., 2015.
487   Electrosprayed nanoparticles and electrospun nanofibers based on natural materials: applications in tissue
488   regeneration, drug delivery and pharmaceuticals. Chem. Soc. Rev. 44, 790-814.
489   Surwase, S.A., Boetker, J.P., Saville, D., Boyd, B.J., Gordon, K.C., Peltonen, L., Strachan, C.J., 2013.
490   Indomethacin: new polymorphs of an old drug. Mol. Pharm. 10, 4472-4480.
491   Verreck, G., Chun, I., Peeters, J., Rosenblatt, J., Brewster, M.E., 2003. Preparation and characterization of
492   nanofibers containing amorphous drug dispersions generated by electrostatic spinning. Pharm. Res. 20, 810-
493   817.
494   Yu, D.-G., Liu, F., Cui, L., Liu, Z.-P., Wang, X., Bligh, S.W.A., 2013a. Coaxial electrospinning using a concentric
495   Teflon spinneret to prepare biphasic-release nanofibers of helicid. RSC Adv. 3, 17775-17783.
496   Yu, D.-G., Shen, X.-X., Branford-White, C., White, K., Zhu, L.-M., Bligh, S.A., 2009. Oral fast-dissolving drug
497   delivery membranes prepared from electrospun polyvinylpyrrolidone ultrafine fibers. Nanotechnol. 20,
498   055104.
499   Yu, D.-G., Williams, G.R., Wang, X., Liu, X.-K., Li, H.-L., Bligh, S.W.A., 2013b. Dual drug release nanocomposites
500   prepared using a combination of electrospraying and electrospinning. RSC Adv. 3, 4652-4658.
501   Yu, D.-G., Xu, Y., Li, Z., Du, L.-P., Zhao, B.-G., Wang, X., 2014. Coaxial electrospinning with mixed solvents:
502   From flat to round Eudragit L100 nanofibers for better colon-targeted sustained drug release profiles. J.
503   Nanomater. 2014, 967295.
504   Zamani, M., Prabhakaran, M.P., Ramakrishna, S., 2013. Advances in drug delivery via electrospun and
505   electrosprayed nanomaterials. Int. J. Nanomedicine 8, 2997-3017.
506   Zupančič, Š., Baumgartner, S., Lavrič, Z., Petelin, M., Kristl, J., 2015. Local delivery of resveratrol using
507   polycaprolactone nanofibers for treatment of periodontal disease. J. Drug Del. Sci. Technol. 30, 408-416.